International Workshop on Nano, Bio and Amorphous Materials

August 9 - 10, 2010

Sansa-tei (Tohgatta, Miyagi-Zao, Japan)

In Association with

- *Highly-functional Interface Science: Innovation of Biomaterials with Highly Functional Interface to Host and Parasite*
- *International Collaboration Center ICC-IMR*
- *Global COE Program "Material Integration" Tohoku University*
- *JSPS 124th Committee on Advanced Ceramics*
- *Division of Functionally Graded Materials, Japan Society of Powder and Powder Metallurgy*

The 5th International Workshop on Nano, Bio and Amorphous Materials

Sansa-tei, Tohgatta, Miyagi, Japan

August 9-10, 2010

PROGRAM

August 9, 2010 (Monday)

15:30 - 15:40 **Opening Address** *Takashi Goto*

15:40 - 16:50 **Project Outlines**

--- Break ---

Keynote Lectures

Chair : Yoshihiro Takao

17:00 - 17:20

Sadami Tsutsumi (Kyoto University)

Regeneration of Periodontal Tissues around Dental Implants

17:20 - 17:40

Akira Yamaguchi (Tokyo Medical and Dental University)

Interface between Cancer and Bone during Bone Destruction by Oral Cancer

17:40 - 18:00

Hideki Hosoda (Tokyo Institute of Technology)

Development of Biomedical Shape Memory Alloys

19:00 - 21:00

Banquet

August 10, 2010 (Tuesday)

Session I - *Chair : Ichiro Takahashi*

09:00 - 09:15

Akihiko Chiba (IMR, Tohoku Univ.)
Damage Processing in a Biomedical Co-29Cr-6Mo-0.14N Alloy Observed by X-Ray Tomography and EBSD

09:15 - 09:30

Hyun-Kwang Seok (Korea Institute of Science & Technology, KIST))
A Suggestion for In-Vitro Cytotoxicity Test Route of Bioabsorbable Mg Alloys

09:30 - 09:45

Jin-Soo Ahn (School of Dentistry, Seoul National University)
Color Change of Layered All-Ceramic Restoration by Dentin Porcelain Thickness

09:45 - 10:00

Takashi Yoshida (Graduate School of Dentistry, Tohoku Univ.)
Mechanosensitive TRP Channels in the Clonal Mouse Osteoblast Cell Line MC3T3-E1

10:00 - 10:15

Tomohiro Masuzaki (Fac. of Dental Science, Kyushu Univ.)
A Single Perilesional Injection of Fluvastatin-PLGA Microspheres Improve Bone Quality around Titanium Implants

--- Break ---

Session II - *Chair : Osamu Suzuki*

10:30 - 10:45

Ichiro Takahashi (Fac. of Dental Science, Kyushu Univ.)
Mechano-Biology of Cytoskeletal Reorganization in Differentiating Chondrocytes

10:45 - 11:00

Mitsuko Kawano (Inst. of Development, Aging and Cancer, Tohoku University)
New Animal Model of Metal Allergy

11:00 - 11:15

Gen Mayanagi (Graduate School of Dentistry, Tohoku Univ.)
Evaluation of pH Using an ISFET at the Parasite-Biomaterial Interface

11:15 - 11:30

Kyosuke Ueda (Department of Materials Processing, Tohoku University)
In Vitro Evaluation of Pack Cementation Treated Titanium Using Tetracalcium Phosphate Powder

11:30 - 11:45

Naru Shiraishi (Division of Advanced Prosthetic Dentistry, Tohoku University)
Biomechanical Evaluation of Calcium Phosphate Films by Radiofrequency Magnetron Sputtering on Different Titanium Implants

Lunch Break

Session III - *Chair : Nobuhiro Takahashi*

13:30 - 13:45

Seung Eon Kim (Korea Institute of Materials Science, KIMS)

3D Scaffolds for Bone Regeneration and Replacement

13:45 - 14:00

Yasuyuki Morita (Graduate School of Engineering, Nagoya University)

Deformation Measurement of Bone Model with a Dental by DIC

14:00 - 14:15

Toshie Kuwana (Graduate School of Dentistry, Tohoku Univ.)

The Influence of Immediate Loading on Bone around Titanium Implants with Different Surface Topographies

14:15 - 14:30

Limei Ren Kyushu Univ.)

Mechanical Analysis of Bone Regeneration Using Porous Bioactive Ceramics

--- Break ---

Session IV - *Chair : Seong- Kyun Kim*

14:45 - 15:00

Zhaoxiang Chen (Kyushu Univ.)

Surface Damage Characterization of Anodized Titanium under Mechanical Loading

15:00 - 15:15

Hiroyasu Kanetaka (Grad. School of Dentistry, Tohoku Univ.)

Application of Ni-free Ti-based Shape Memory Alloy for Maxillofacial Treatment

15:15 - 15:30

Qiang Li (IMR, Tohoku Univ.)

Aging Behavior of β-type Ti-37Nb-3Zr with Super-elasticity

15:30 – 15:45

Albertus D. Setyawan (IMR, Tohoku Univ.)

Glass-Structure Control in Zr-based Metallic Glasses by Varying Casting Atmosphere Condition

15:45 – 15:55 **Closing Remarks** *Keichi Sasaki*

“Regeneration of Periodontal Tissues around Dental Implants”

Sadami TSUTSUMI, Dr.Eng., Professor Emeritus at Kyoto University

Synopsis: A trial of PDL (periodontal ligament) around a dental implant was carried out by culturing PDL cells on a EVA coated titanium implant in order to require the functional recovery of the dental implant. The hybrid implant was prepared as follows; The titanium implant was oxidized by hydrogen peroxide. EVA was coated onto the implant and oxidized with ozone gas to introduce carboxyl groups on the surface. The collagen sponge was immobilized around the implant by a freeze-drying method, followed by PDL cell culture onto the implant for 14 days. Then, the cell-seeded implant was applied to the implantation in a canine alveolar bone with a biodegradable membrane that was to prevent a downgrowth of epithelial cells. After 3 months of the implantation, the implants and their surrounding tissue were recovered and the histological analyses were performed. The collagen fibers around the hybrid implant were seemed to be vertically to the alveolar bone similar to those around a natural tooth. Regenerated PDL were seen in around 30 % of the root part of the hybrid implant, suggesting a possibility of the regeneration of PDL around itself.

Interface between cancer and bone during bone destruction by oral cancer

Akira Yamaguchi

Section of Oral Pathology, Graduate School of Medical and Dental Sciences, Tokyo Medical and Dental University, Global Center of Excellence Program, International Research Center for Molecular Science in Tooth and Bone Diseases, Tokyo Medical and Dental University

akira.mpa@tmd.ac.jp

Oral squamous cell carcinoma (OSCC) frequently invades the jaws, and this invasion is associated with a worse prognosis. Although previous studies have suggested that bone destruction caused by OSCC is mediated by osteoclastic bone resorption, the mechanism underlying the bone invasion remains poorly understood. We histopathologically investigated mandibular invasion patterns in 97 cases of primary OSCC. We found that tumor cells showed no direct contact with osteoclasts and the adjacent bones, and in all cases varying amounts of fibrous connective tissues intervened between the tumor cells and the bone. We also found a positive correlation between the number of osteoclasts and fibroblasts at the interface of the tumor and the resorbing bone. Immunohistochemistry revealed RANKL expression in the fibroblastic cells that were adjacent to the osteoclasts in the area of bone resorption [1]. These results suggest that the fibrous stroma is involved in osteoclastic bone resorption. To explore the molecular mechanism, we investigated the roles of IL-6 and parathyroid hormone-related peptide (PTHrP) in OSCC-induced osteoclast formation [2]. Microarray analyses performed on 43 human OSCC specimens revealed that many of sp ecimens overexpressed *PTHrP* mRNA, but a few overexpressed *IL-6* mRNA. Immunohistochemical analysis revealed that IL-6 was expressed not only in cancer cells but also in fibroblasts and osteoclasts at tumor-bone interface. Conditioned media (CM) derived from the culture of oral cancer cell lines (BHY, Ca9-22, HSC3, HO1-u-1) stimulated *Rankl* expression in stromal cells and osteoclast formation. Antibodies against both human PTHrP and mouse IL-6 receptor suppressed *Rankl* in ST2 cells and osteoclast formation induced by CM from BHY and Ca9-22, although the inhibitory effects of IL6 antibody were greater than those of PTHrP antibody. CM derived from all of the OSCC cell lines effectively induced IL-6 expression in stromal cells, and the induction was partially blocked by anti-PTHrP antibody. Xenografts of HSC3 cells onto the periosteal region of the

parietal bone in athymic mice presented similar histology and expression profiles of RANKL and IL-6 as observed in bone-invasive human OSCC specimens. These results indicate that OSCC provides a suitable microenvironment for osteoclast formation not only by producing IL-6 and PTHrP but also by stimulating stromal cells to synthesize IL-6.

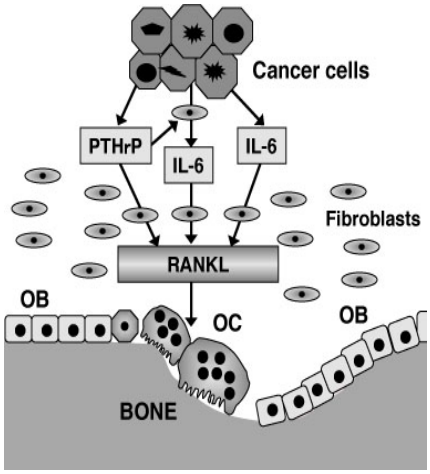

References

1. Ishikuro M, Sakamoto K, Kayamori K, Izumo T, Yamaguchi A: Role of fibrous stroma in bone invasion by gingival squamous cell carcinomas. ***BONE*** 43:621-627,2008
2. Kayamori K, Sakamoto K, Nakashima T, Takayanagi T, Morita K, Omura K, Nguyen ST, Miki Y, Iimura T, Himeno A, Akashi T, Yamada-Okabe H, Ogata E, Yamaguchi A: Roles of IL-6 and PTHrP in osteoclast formation associated with oral cancers: The significance of IL-6 synthesized by stromal cells in response to cancer cells. ***Amer J Pathol*** 176, 968- 980, 2010

Development of Biomedical Shape Memory Alloys

Hideki Hosoda

Precision and Intelligence Laboratory, Tokyo Institute of Technology,
4259-R2-27 Nagatsuta, Midori-ku, Yokohama 226-8503, Japan
phone&fax: +81-(0)45-924-5057, email: hosoda.h.aa@m.titech.ac.jp

Shape memory effect (SME) and superelasticity (SE) become much important for advanced biomedical applications such as guide wires, stents, catheters and orthodontic wires. Today, Ti-Ni shape memory alloy (SMA) is only one practical biomedical SMA. However, the possibility of Ni-hypersensitivity is concerned and Ni-free, rather, toxic-element-free biocompatible SMAs are required. Besides, as for the implant medical device materials such as stents, X-ray radiography is important. Ti-Ni SMA exhibits, however, poor X-ray radiography since both Ti and Ni belong to the 3d transition metal group. Based on the backgrounds, we have conducted to develop two types of Ni-free biomedical SMAs. One is classified into β titanium alloys and the other is gold base alloys. This presentation describes the recent topics of development of biomedical SMAs obtained by our group.

Many titanium alloys exhibit nonthermoelastic martensitic transformation from β to α'. If the alloys contain a proper amount of β stabilizer such as Nb and Mo, a thermoelastic martensitic transformation from β to α" is stabilized and SME appears. Now several kinds of Ni-free Ti-based SMAs have been reported. For example, Ti-24Nb-3Al (mol%) alloy exhibits good SE around 6% in total strain. The lowest Young's modulus reaches to 29GPa which is comparable to human bone. The biocompatibility is better than that of Ti-Ni. A drawback for practical applications is imperfect shape recovery obtained for the solution-treated (ST) alloys. Then, a proper shape memory treatment should be achieved. Figure 1 shows a trial for seeking a proper thermo-mechanical treatment. TiMoAl biomedical SMA exhibited SME after ST at 1273K for 3.6ks. When the material was aged at 623K, pseudoelasticity appeared. When the aging temperature is slightly increased to be 773K, the material was brittle due to ω embrittlement. However, when a three step aging of 773K-1023K-1123K was carried out, the material exhibited high strength and perfect shape recovery.

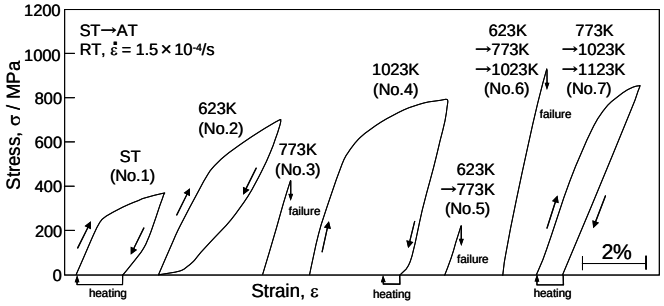

Figure 1 Stress-strain curves of Ti-6Mo-8Al (mol%) biomedical SMA after single- and multi-step aging.

AuTi is a high temperature SMA with M_s being 880K. We found that Co addition decreases M_s of AuTi, and M_s becomes the body temperature by 18~19mol%Co addition. However, the ST alloy did not exhibit SE and relatively brittle. When aging at 573K for 3.6ks was carried out, SE clearly appeared and mechanical properties were improved. Then, AuTiCo is a good candidate for implant applications. Besides, aging treatment is important for SMAs.

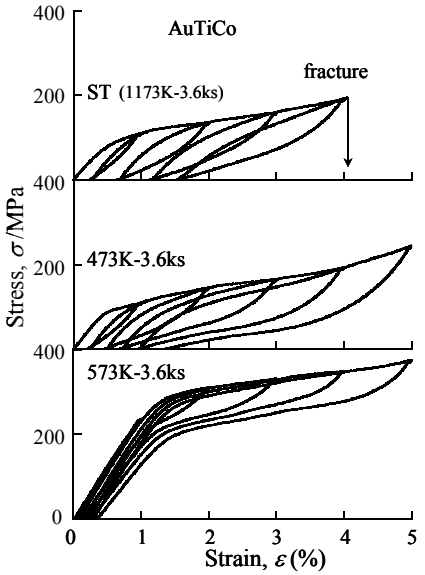

Figure 2 Stress-strain curves of AuTiCo with various heat treatments.

Damage Processing in a Biomedical Co-29Cr-6Mo-0.14N Alloy Observed by X-Ray Tomography and EBSD

Shingo Kurosu, Hiroaki Matsumoto, Akihiko Chiba
Institute for Materials Research, Tohoku University
a.chiba@imr.tohoku.ac.jp

Co-Cr-Mo alloys represent the most important category of metallic biomaterial for surgical implant applications **[1-3]**.When nitrogen is added, Co-Cr-Mo alloys exhibit a metastable γ-fcc structure. However, the Co-Cr-Mo alloy with nitrogen addition exhibits limited cold-workability despite the good elongation shown at room temperature. This is due to the fact that the alloys show significant low stacking fault energy (SFE) as compared with conventional low SFE alloys, such as austenitic stainless steel and the Co-Cr-Mo alloy with addition of nickel.

Many investigators have used both XRD analysis and SEM observation of fractured specimens to reveal the damage process of the Co-Cr-Mo alloys. However, these postmortem analyses give limited information about the damage process because coming from the surface, while damage process in the bulk is not clarified yet. X-ray tomography is very attractive technique which enables the in situ observation of internal features during tensile testing and therefore can provide information about the three-dimensional damage process, including occurrence of dimple, crack initiation and propagation in the bulk.

The main interest in the present study was to characterize three-dimensional (3D) damage process during tensile testing in the biomedical Co-29Cr-6Mo-0.14N alloy using X-ray tomography. The fracture process of the present alloy was analyzed on the basis of the 3D observation of damage combined with EBSD analysis of the fractured specimen.

The specimen for tomography was machined along parallel to swaging direction. The specimen for X-ray tomography was a semi-circularly notched round bar (diameter: 3 mm). The notch radius was set to 1mm. The X-ray tomography used is the one available at the European Synchrotron Radiation Facility (ESRF) in Grenoble, France on the ID15 beam-line. It achieves a fast radiography acquisition speed by combining a high-efficiency scintillator screen, reflecting microscope objective and a fast charge-coupled device detector with a very intense high-energy white beam radiation produced by a wiggler source. An in situ tensile device described in Ref **[16]** was mounted on the rotation stage of the tomography setup. The detail experimental conditions were the following: white X-ray radiation with a peak energy set to 50 keV, number of projections 500, and time for recording one projection 150 ms.

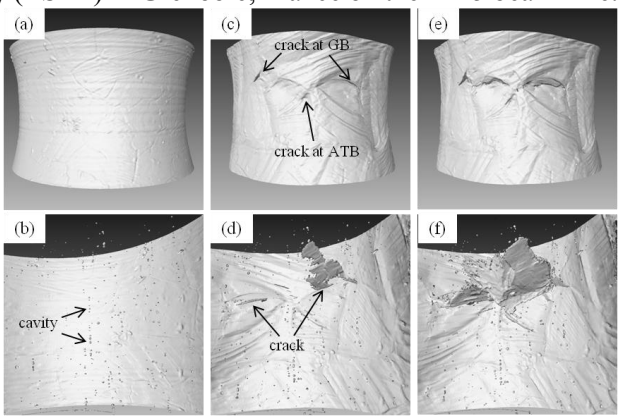

Fig.1 3D tomographic reconstruction of Co-29Cr-6Mo-0.14N alloy at three different relevant damage steps: (a), (b) initial state; (c), (d) crack initiation state and (e), (f) the state just before fracture. Fig. 1 (a), (c), (e) and (b), (d), (f) indicate the outer surface and the inner cracks inside the specimen, respectively.

Figure 1 shows a 3D tomographic reconstruction of Co-29Cr-6Mo-0.14N alloy at three different relevant deformation steps: (a), (b) initial state (undeformed); (c), (d) crack initiation state and (e), (f) the state just before fracture. Fig. 1 (a), (c), (e) and (b), (d), (f) show the outer surface together

with the inner cracks inside the specimen, respectively. In the initial state, the surface is shown to be smooth and one cannot distinguish the grains and their boundaries (Fig. 1(a)). Some cavities are present in the undeformed state (Fig. 1(b)). According to XRD analysis and microstructural observation, no precipitates were confirmed in the initial microstructure. Therefore, it is suggested that these cavities may originate from nitrogen gas pore during casting process, since the fall in straight line along parallel to swaging direction and disappeared after swaging process. When specimens were elongated (Fig. 1(c)), their grains began to deform differently due to the grain orientation of each grain interacting with its neighbors. Therefore, grain boundaries (GBs) and annealing twin boundaries (ATBs) can be observed clearly. Additionally, some slip bands appear inside each grain. Cracks are observed to initiate at GBs and ATBs at the surface of the sample while no cracks are detected inside. As the tensile test proceeds, the crack developed along the boundaries (Fig. 1(c)) and propagated towards the inside of the specimen (Fig. 1(d)). Finally, transgranular cracking occurred and coalesced with the intergranular crack (Fig. 1(e)). Moreover, it can be observed that transgranular cracking propagates along specific habit plane (Fig. 1(f)). In contrast, it is observed that the cavities which existed in the initial state do not grow substantially during tensile testing. Thus the original cavities do not strongly modify the fracture behavior in the present alloy. Therefore, it is found that the material under study shows a specific fracture process, instead of the general fracture process observed in most ductile metals (nucleation, growth and then coalescence of the cavities **[14-16]**).

On the basis of the results mentioned above, a scenario for the fracture process in the Co-29Cr-6Mo-0.14N alloy with coarse grains is proposed as schematically shown in the **Figure 2;** (a) undeformed state, (b) initial deformation, (c) crack initiation and (d) fracture. In Fig. 4(b), prior to crack initiation, some slip bands appear within each grain. The slip bands probably corresponding to dense SFs that are namely nuclei of SIMTed ε or thin SIMTed ε plates created by the movement of partial dislocation since the Ni-free Co-Cr-Mo alloys have a significant low SFE. Thus, in the case of the present alloy, SIMT might be triggered by relatively small amounts of strain. In Fig. 4(c), the initial cracking occurs at GBs including ATB on the surface of the specimen. The SIMTed ε plates can intersect each other. Therefore, strain concentration is expected to occur at the GBs and ATBs, on which the SIMTed ε plate impinged, but not at the intersection between SIMTed ε plates. In Fig. 4(d), strain concentration occurs at the interface between original γ and SIMTed ε plate on {111} including ATBs. Transgranular cracking propagates along their interface and coalesces into the intergranular crack, resulting in the occurrence of quasi-cleavage fracture along {111}.

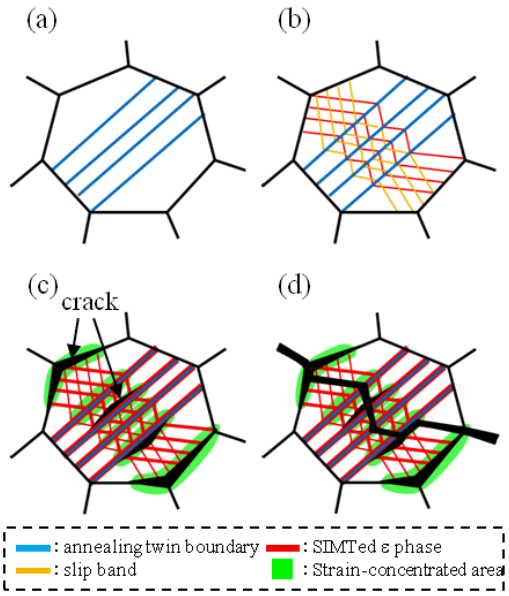

Fig. 2 Schematic illustrations of the fracture process in the Ni-free Co-29Cr-6Mo-0.14N alloy with coarse grains.

A Suggestion for in vitro cytotoxicity test route of bioabsorbable Mg alloys

Hyun-Kwang Seok[1], Yu-Chan Kim[1,2], Hee-Kyoung Kim[1], Sung-Youn Cho[3], Young-Yeoul Kim[4], Seok-Jo Yang[5]

[1] Division of materials, Korea Institute of Science & Technology, Seoul 136-650, Korea
[2] Biomaterials Center, NIMS, Japan
[3] Div. of Orthopedic, Catholic Univ., Deajeon, Korea
[4] U&I Inc., Uijong bu, Kyung Gi Do, Korea
[5] Depart. of Mechatronics Eng., Chungnam Nat. Univ., Deajeon 305-764, Korea

A new domain of research in metallic implants focuses on biodegradable implants, which dissolve in biological environment after a certain time of functional use. Biodegradable implants represent an appropriate solution because of cost, convenience and aesthetic reasons favorable to patients. Magnesium as a biodegradable implant material provides both biocompatibility and suitable mechanical properties. Mg^{2+} ion is present in large amount in the human body, being involved in many metabolism reactions and biological mechanisms, and Mg^{2+} in excess can be easily excreted in the urine. Moreover, compared to current implant materials, magnesium and magnesium-based alloys have a lower elastic modulus (about 45 GPa which is closed to that of natural bone (10–40 GPa)) and a higher yield strength, that provide them with the potential for avoiding the stress shielding effects. Thus, it is projected that magnesium and its alloys be applied as lightweight, degradable, load bearing orthopedic implants, which would remain present in the body and maintain mechanical integrity over a time scale of 12-18 weeks while the bone tissue heals, eventually being replaced by natural tissue.

Cytotoxicitiy test route of biomaterials is regulated on ISO rule book(regulation; 10993-5). However, for the cytotoxicity evaluation of bioabsorbable Mg alloys, increase of both pH and Mg^{2+} ion contents should be considered all together, which cannot be done following previous ISO 10993 rule because there is no suggestion how to simulate the pH variation during implantation of Mg alloys into body. In this study, the effect of pH control in cytotoxicity test of Mg alloy was investigated by adding additional acid in media during/after extraction and by artificial pH regulation through CO_2 blowing onto the media. Also, the effect of ions on the cytotocity of the bioabsorbable material has been observed by adding metal ions under considering into the media. From the experimental results, increase of pH decreased cell viability in direct and/or indirect manner. Even by regulation of pH of cell culture media as 7.4 after extraction step, the cell viability was very low, which was caused by protein changes by pH increase during extraction stage. However, pH regulating through CO_2 blowing onto the media during extraction stage sustained the pH lower than 8.0 and resulted in better cell viability. Therefore it was concluded that proper route should be proposed for simulating pH regulation in human body via in vitro cytotoxicity test method.

The authors acknowledge the support by the KIST project(2E21860).

Color change of layered all-ceramic restoration by dentin porcelain thickness

Jin-Soo Ahn[1*], Seong-Kyun Kim[2*]
[1]*Department of Dental Biomaterials Science,* [2]*Department of Prosthodontics,*
**Dental Research Institute, School of Dentistry, Seoul National University, Seoul, Korea*
ahnjin@snu.ac.kr

Objectives: All-ceramic restorations can be made to match natural tooth color and translucency through the layering of core and veneer ceramics of varying translucency, shade, and thickness. However, clinical shade matches are typically hard to achieve, even when an adequate ceramic thickness exists [1]. Therefore, clinicians must recognize the effects of core and veneer ceramics on the final layered color, in order to effectively implement the layering technique for strong and cosmetically acceptable all-ceramic restorations [2]. This study aims to identify and quantify the effect of increased dentin porcelain thickness on the color and color coordinates of all-ceramic specimens.

Methods: Zirconia (Lava) and Lithium Disilicate (IPS e.max Press) all-ceramic systems were investigated. A1, A2 and A3.5 shades of layered specimens were made with 2-mm ceramic cores and 0-to-2 mm beveled dentin porcelain. Color was measured at 0.25 mm intervals along the specimen surface with a spectroradiometer. The effect of ceramic brand, shade and dentin porcelain thickness on color change was analyzed by 3-way ANOVA.

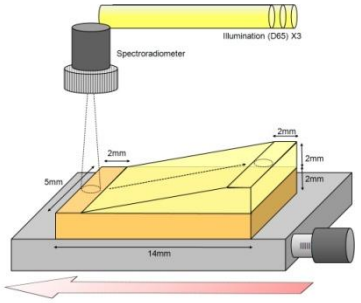

Fig. 1 Schematic representation

Results: Color changes of layered ceramics varied by ceramic brand, shade and dentin porcelain thickness. For most ceramics, the CIE a^*, b^* and C^*_{ab} values gradually increased as the thickness of the dentin porcelain increased. Conversely, such increases in dentin porcelain thickness were correlated with decreasing CIE L^* values. When compared with the IPS e.max Press ceramics, Lava ceramics showed smaller color changes in response to increases in dentin porcelain thickness.

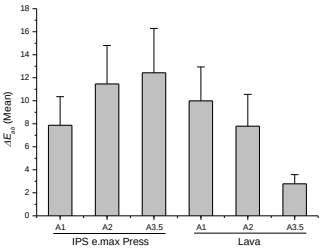

Fig. 2 Mean color differences

Conclusions: The final appearance of ceramic restorations can be manipulated by varying the dentin porcelain thickness. However, the color and color coordinate of the layered ceramics vary by ceramic brand, shade and dentin porcelain thickness.

References:

1) Douglas RD, Przybylska M. Predicting porcelain thickness required for dental shade matches. *Journal of Prosthetic Dentistry* 1999;**82**:143-9
2) Lee YK, Cha HS, Ahn JS. Layered color of all-ceramic core and veneer ceramics. *Journal of Prosthetic Dentistry* 2007;**97**:279-86

Mechanosensitive TRP channels in the clonal mouse osteoblast cell line MC3T3-E1.

Takashi Yoshida[1], Minoru Wakamori[1]

1 Div. Mol. Pharmacol. and Cell Biophys., Dept. Oral. Biol. Tohoku univ. Grad. Sch. Dent. t-yoshida@mail.tains.tohoku.ac.jp

Mechanical loading is essential for maintaining skeletal integrity and bone mass. Osteoblasts lining the endosteal and periosteal surfaces of bone have been shown to be sensitive to mechanical loading. It has been shown that mechanical stimuli regulate various osteoblast functions, including gene expression, protein synthesis, cell proliferation and cell differentiation. The earliest cellular response detected in mechanically stimulated osteoblasts is an increase in intracellular calcium concentration ($[Ca^{2+}]_i$). This increase in $[Ca^{2+}]_i$ results from Ca^{2+} influx from the extracellular space via calcium channels located on the plasma membrane. In spite of the significant role of calcium channels in osteoblast, the molecular identity of mechanosensitive channels remains unknown. To identify the mechanosensitive channels, we examined the expression level of mammalian homologues of *Drosophira* transient receptor potential (TRP) channel superfamily in the clonal mouse osteoblast cell line MC3T3-E1. Recently, several members of the TRP family of cation channels have been proposed as mechanosensitive ion channels [1]. Mechanosensitive TRP channels are mainly investigated in the cardiovascular system. In artery myocytes, TRPM4 and TRPV2 cation channels are activated by membrane stretch. TRPV4 and TRPM7 have been reported that cell swelling activates these channels and induces Ca^{2+} influx. The flow-mediated Ca^{2+} transient requires the presence of functional TRPP2 and TRPP1. Using RT-PCR, we detected signals for some TRP channels belong to TRPV and TRPM subfamilies in osteoblastic cell. In members of TRPV subfamily, TRPV2 and TRPV4 mRNAs were expressed. Channels of TRPM subfamily, TRPM7 mRNA was found at highest levels. TRPM3 and TRPM4 mRNA were found at significant levels. In addition, strong signals were found for TRPP1 and TRPP2 in our survey using MC3T3-E1 cells. Based on these results we propose that TRP channels are important candidate of mechanosensitive channels in MC3T3-E1 cells.

1. Pedersen SF, Nilius B (2007) Transient receptor potential channels in mechanosensing and cell volume regulation. Methods Enzymol 428:183-207.

A single perilesional injection of fluvastatin-PLGA microspheres improve bone quality around titanium implants

Tomohiro Masuzaki, Yasunori Ayukawa, Yohei Jinno, Kiyoshi Koyano
Section of Implant & Rehabilitative Dentistry, Division of Oral Rehabilitation, Faculty of Dental Science, Kyushu University
masuzaki@dent.kyushu-u.ac.jp

Objectives: Dental implants are increasingly becoming one of major treatment modalities for the rehabilitation of missing teeth with high predictability. However, it needs enough bone quality and good bone quantity. There have been reported a lot of methods to increase bone quality, but effective methods for the improvement of bone quality have scarcely been reported.

Statins are cholesterol-lowering drugs that inhibit 3-hydroxy-3-methylglutaryl-coenzyme A (HMG-CoA) reductase and recent studies show that statins enhance bone formation in vivo and in vitro. When statins administrated orally, it need very large doses. But if it administrated locally or subcutaneously without carrier, it was metabolized in short period. So we selected microsphere-shaped biodegredable poly (lactic-co-glycolic acid) (PLGA) for sustained release carrier. The aim of this investigation was to evaluate the effect of newly-developed injectable PLGA microspheres containing fluvastatin on the osteogenesis around the titanium implant inserted into rat tibia.

Methods: We prepared fluvastatin-impregnated PLGA microspheres by an in-water drying method and checked the sustained-release of fluvastatin from microspheres by a vitro assay. Titanium implants are inserted into rat tibia, and microspheres were administrated in the vicinity of the implant. The groups were divided into four, namely, control (none), PLGA only, PLGA containing fluvastatin 0.25mg/kg or 0.5mg/kg. At 2 and 4 weeks after the implant surgery, histomorphometrical evaluation, serum biochemistry, bone metabolism marker, and biomechanical testing of femurs were conducted.

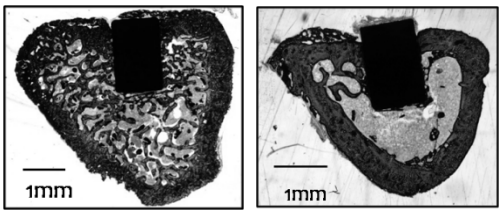

Results: At 2 and 4 weeks after the implant surgery, statin groups were significantly enhanced new bone formation around titanium implants without any influence on serum biochemical value. In addition, PLGA/fluvastatin significantly increased the three-point bending strength of the femur. ($p<0.05$, ANOVA)

Conclusion: This study indicated that a single perilesional injection of PLGA/fluvastatin enhanced bone formation around titanium implants in rat tibia and improved the femoral bone strength, without any influence on the serum biochemistry.

Mechano-biology of cytoskeletal re-organaization in differentiating chondrocytes

Ichiro Takahashi[1], Taisuke Masuda[2], Kumiko Kohsaka[3], Fumie Terao[3], Takahisa Anada[2], Yasuyuki Sasano[4], Teruko Takano-Yamamoto[3], Osamu Suzuki[2]

[1]*Section of Orthodontics, Kyushu University Faculty of Dental Science,*
takahashi@dent.kyushu-u.ac.jp
[2]*Dept. of Mechanical Science and Engineering,*
Nagoya University Graduate School of Engineering
[3]*Division of Orthodontics and Dentofacial Orthopedics,*
[4]*Division of Craniofacial Function Engineering,*
[5]*Division of Craniofacial Development and Regeneration,*
Tohoku University Graduate School of Dentistry

Mechanical stress is considered to be one of the key stimulating factors regulating the differentiation of mesenchymal cells in the skeletal tissues as well as growth factors and cytokines. In the skeletal tissues, cartilages and bones are loaded mechanical stress by body action and functions, and respond to them by changing metabolism and differentiation status resulting in the shape and size of skeleton. Mechanical stress could be transferred from the extracellular matrix (ECM) through cell-ECM adhesion to nucleus of cells to regulate the gene expressions. Cartilage develops from cellular condensation mesenchymal stem cells during early stage of embryonic development with undifferentiated ECM molecules such as tenascin, fibronectin, type III collagen and type I collagen. Cell-ECM adhesion complex formed between these molecules and fibronectin receptors changes to cell-ECM adhesion between cartilaginous unique ECM composed of collagens and proteoglycans and their recptors including other type of integrins as the chondrocyte differentiates.

In vivo, we found that the progenitor cells in the midpalatal suture cartilage in rats responded to tesile stress by de-differentiating, while they differentiate into chondrocyte and further to hypertrophic chondocytes under the compressive loading. In vitro, mechanical compressive stress, indeed, accelerated chondrogenic differentiation of mesenchymal stem cells derived from embryonic limb bud, while tensile stress inhibited the chodrogenesis from same cell source. Specifically under tensile stress, differentiating chondrocytes responded to mechanical tensile force by altering their cell shape and cytoskeleton (Figure 1) accompanied with activation of mitogen-activated protein kinase pathway through extracellular signal-regulated kinase (ERK)-1/2. Here, we show the roles of cell-ECM adhesion through integrin on the mechanical stress response in chondrocytes and demonstrate the direct up-regulation of ERK phosphorylation under the control of mechanical stretch and cytoskeletal morphological changes under the control of Rho GTPase. While activation of ERK peaked in 60 min after mechanical stretch loading, activation of Rho GTPase reached to the peak in 15 min. Thus, cell shape change during mechano-response of chondrogenesis could precede to the mechano-transduction of stretch stimulation via ERK-1/2 signaling pathway.

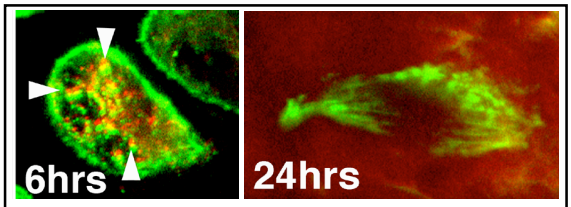

Figure 1. Cell shape change after stretch stimulation was accompanied with stress fiber formation.

Thus, differentiating chondrocytes respond to mechanical stress by altering their shape and phenotypes. It could be considered that the size and shape of the skeleton is affected by the mechanical stress loaded on skeletal tissue, such as bone and cartilage.

New animal model of metal allergy

Mitsuko Kawano, and Kouetsu Ogasawara

Department of Immunobiology, Institute of Development, Aging and Cancer, Tohoku University

The patients of metal allergy have greatly increased because the metal materials for jewelry and medical treatments are widely used. In addition, related diseases of metal allergy are generally incurable, therefore, severely hindering the patient's quality of life. However, the problems are not to be addressed.

From the clinical point of view, although patch testing is effective to diagnose metal allergy, it is difficult for clinician to diagnose metal allergy and it might be sensitized to patients for diagnosis. Therefore, the patients as well as the clinician are desired a more effective diagnostic method. Furthermore, from the scientific point of view, metal allergy has been characterized as type IV allergy which is T cell dependent diseases by the studies of allergic patients. Nevertheless, the time series of disease development for metal allergy and molecular mechanisms of the disease are still unknown because the appropriate animal model has not been established.

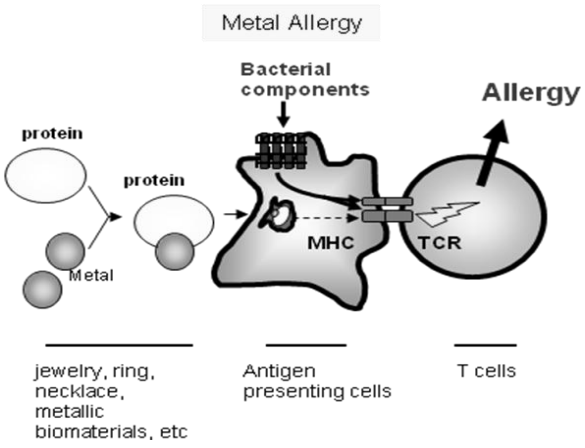

Thus, to examine the molecular mechanisms underlying the disease development of metal allergy, we attempted to establish a new animal model. Mice were injected bacterial components with metal solution into intra-peritoneally for sensitization. 7 days later, metal solution was injected into dermis of the ear. Ear swelling and inflammation were observed. Lymphocytes also accumulate in the lesion of the ear. That seems to be the specific symptoms of metal allergy. Furthermore, we found that the disease developed in nude mice by the transfer of T cells derived from sensitized mice by metal.

These results indicated that T cells are critical for the development of metal allergy in animal model.

Evaluation of pH using an ISFET at the parasite-biomaterial interface

Gen Mayanagi[1,2], Koei Igarashi[2], Jumpei Washio[2], Kazuko Nakajo[2],
Hitomi Domon-Tawaraya[2] and Nobuhiro Takahashi[2]
[1] *Research Unit for Interface Oral Health Science,*
[2] *Division of Oral Ecology and Biochemistry, Department of Oral Biology,*
Tohoku University Graduate School of Dentistry, Sendai, Japan
genm@mail.tains.tohoku.ac.jp

Introduction

Physiochemical assessment of the parasite-biomaterial interface is essential when developing new biomaterials, particularly for use in the oral cavity. The purpose of this study was to develop a method to evaluate pH at the parasite-biomaterial interface and demonstrate physiochemical interaction at the interface.

Materials and Methods

Representative three conventional dental cements (glass-ionomer (GIC), zinc phosphate (ZPC) and zinc oxide-eugenol (ZOE) cements) were used in the present study. Disk specimens of dental cements (8.0-mm in diameter, 2.0-mm in thickness) were prepared according to manufacturer's instructions. Each specimen was immersed in 2 mM potassium phosphate buffer (PPB) at 37°C for 10 min, 24 h, 1 week or 1 month. An experimental chamber for pH monitoring (4.0-mm in diameter and 2.0-mm in depth) was made of acrylic resin with a bottom of dental cement. The well was filled with cells of *Streptococcus mutans* NCTC 10449 (SM), and an ion-sensitive field-effect transistor (ISFET) was placed at an interface between SM cells and dental cement. The pH was monitored after the addition of 1% glucose at 37°C. Amounts of fluoride in the SM cells and the PPB used for cement immersion were measured using a fluoride ion electrode.

Results and Discussion

The pH at SM cells-biomaterial interface was successfully monitored using the experimental chamber with an ISFET. GIC inhibited the pH fall by bacterial sugar fermentation at the interface, whereas ZPC and ZOE had no inhibitory effects. The pH of SM cells-GIC interface at 90 min was significantly higher ($p < 0.01$) than that of SM cells-acrylic resin interface (control), regardless of immersion time. Significant higher amounts of fluoride ($p < 0.05$ or 0.01) were detected in the SM cells after sugar fermentation for 90 min, suggesting that the inhibitory effect was mainly due to the fluoride released from GIC during glucose fermentation. This method using ISFET could be useful to assess the pH at the parasite-biomaterial interface.

In vitro evaluation of pack cementation treated titanium using tetracalcium phosphate powder

Kyosuke Ueda[1)], Kaori Nakaie[1)], Hajime Suto[1)], Takayuki Narushima[1)] and Masayuki Taira[2)]
[1)]*Department of Materials Processing, Tohoku University*
[2)]*Department of Dental Materials and Technology, Iwate Medical University School of Dentistry*

1. Introduction Calcium phosphate coating on titanium is one of the useful techniques to improve the bone compatibility. Pack cementation treatment using calcium phosphate powder is a new process that is being used to form a bioactive reaction layer on titanium materials[1)]. In this study tetracalcium phosphate ($Ca_4(PO_4)_2O$, TTCP) slurry was used for the treatment, and the phase and morphology of the reaction layer were investigated. The bonding strength, apatite formation ability and alkaline phosphatase (ALP) activity of the reaction layers were evaluated.

2. Experimental A mirror-polished commercially pure titanium (CP Ti) plate (10×10×1 mm) was used as the substrate. TTCP slurry for the treatment was prepared by mixing TTCP powder with deionized water. The substrate was embedded in the TTCP slurry in an Al_2O_3 crucible and heat treated at 973 K in air. After pack cementation treatment, the substrate was ultrasonically cleaned using ethanol and deionized water. The phase, chemical composition and morphology of the reaction layer were examined. The bonding strength between the reaction layer and the substrate was evaluated using a mechanical strength tester. Apatite formation ability of the reaction layer was evaluated by the immersion test in Kokubo solution. SaOS-2 cells were cultured and the ALP activity of the treated and non-treated substrates was evaluated.

3. Results and discussion Hydroxyapatite ($Ca_{10}(PO_4)_6(OH)_2$, HAp), $CaTiO_3$ and rutile phases were observed after the pack cementation treatment using TTCP slurry at 973 K for 86.4 ks. The decomposition reaction of TTCP to HAp and CaO was occurred, and the CaO would react with TiO_2 to form the $CaTiO_3$. Figure 1 shows the SEM images of the surface and cross section of the reaction layer after pack cementation using TTCP slurry. The HAp particles and pores with a diameter of several micrometers were observed. The reaction layer consisted of inner and outer layers. The oxide layer formed by the outward diffusion of Ti caught particles, and these particles were trapped in the pores on the inner reaction layer. The detachment of particles during the removal of the packed powder after pack cementation treatment caused the formation of pores. The bonding strength between the substrate and the reaction layer, having a total thickness of 1.4 μm, obtained by pack cementation treatment at 973 K for 21.6 ks was 68.1 MPa. This value was greater than that of the plasma-sprayed calcium phosphate coating film. Small apatite crystallites were uniformly observed on the surface of the treated substrate after 10.8 ks, and the specimens were completely covered with apatite after immersion for 21.6 ks. The ALP activity of the treated substrate was greater than that on the non-treated substrate.

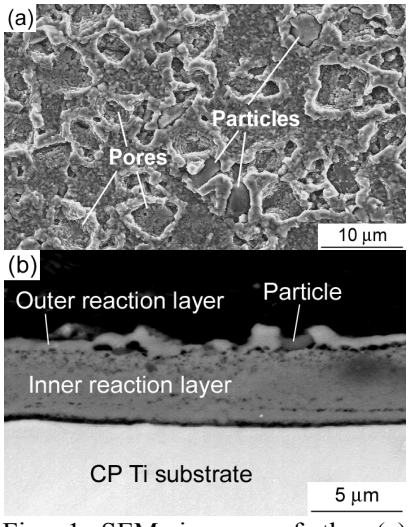

Fig. 1 SEM images of the (a) surface and (b) cross section of the reaction layers on CP Ti substrates after pack cementation using TTCP slurry at 973 K for 86.4 ks.

[1)]K. Ueda, H. Suto and T. Narushima: Met. Mater. Int. accepted.

Biomechanical Evaluation of Calcium Phosphate Films by Radiofrequency Magnetron Sputtering on different Titanium Implants

Naru Shiraishi[1, 2], Yuko Suzuki[1], Naoko Sato[1], Takashi Goto[3], Rong Tu[3], Niinomi Mituo[4], Takayuki Narushima[5], Kyosuke Ueda[5], Risa Uzuka[1], Osamu Suzuki[2] and Keiichi Sasaki[1]

[1]*Division of Advanced Prosthetic Dentistry, Tohoku University*

[2]*Division of Craniofacial Function Engineering (CFE), Tohoku University*

[3]*Department of Multi-Functional Materials Science, Institute for Material Research (IMR), Tohoku University*

[4]*Department of Biomaterials Science, Institute for Material Research (IMR), Tohoku University*

[5]*Department of Materials Processing, Tohoku University*

nshiraishi@mail.tains.tohoku.ac.jp

Introduction

Dental implant treatments have become a major reconstructive method for edentulous site. In implant treatment, osseointegration (implant-tissue direct integration) is essential phenomenon found in titanium-bone intersurface. To improve biocompatibility of titanium alloys with bone, we fabricated the implants coated with amorphous calcium phosphate (ACP) by Radiofrequency (RF) magnetron sputtering system.

Materials and Methods

In this study, miniature cylindrical implants (2.0 mm high, 1.0 mm diameter) made from commercially pure Titanium (cpTi) and Ti-29Nb-13Ta-4.6Zr alloys (TNTZ) were used. On these implants surfaces, ACP film was fabricated using a RF magnetron sputtering system with β-TCP targets. Four types of these implants were prepared for a biomechanical push-in test. Ten-week-old Sprague-Dawley rats were used, and two implants per femur were placed 7 and 11 mm from distal end of the femur. Animals were killed at weeks 2 and 4 of healing period. Femurs were harvested and embedded in autopolymerizing resin, and then push-in test was carried out. A pushing rod was used to load the implant vertically downward at a crosshead speed of 1 mm/min. The peak of the load-displacement curve was measured as push-in value. After the push-in test, the implant surfaces were observed by scanning electron microscopy (SEM).

Results and Discussion

At 2 weeks, the push-in value of ACP-cpTi and ACP-TNTZ are almost the same. At 4 weeks, the value of ACP-TNTZ is higher than that of ACP-cpTi. These results may be due to the difference between of characteristics of ACP on the cpTi and those of TNTZ.

3D Scaffolds for Bone Regeneration and Replacement

Seung Eon Kim*, Hui Suk Yun, Yong Taek Hyun

Korea Institute of Materials Science (KIMS),
797 Changwondaero, Sungsangu, Changwon, Gyeongnam 641-831, Korea
* sek24@kims.re.kr

The scaffolds for tissue regeneration or replacement should be porous enough to provide tissue in-growth. Several routes have been so far employed to fabricate porous scaffolds, such as particulate leaching, solvent casting, freeze drying, gas foaming, electrospinning and so on. However, insufficient interconnectivity of the pores in the conventionally fabricated scaffolds has often resulted in poor cell or tissue permeability, especially in case of large scaffolds. Further, those conventional processes might have some weaknesses in reproducibility, reliability, standardization for commercialization. Meanwhile, the layer manufacturing technology has been spotlighted as a prospective scaffolding process to overcome those roadblocks, owing to three dimensionally(3D) controlled designing and shaping of pore structure by computer aided program.

In past years, we have studied a layer manufacturing process to fabricate porous 3D scaffolds for bone regeneration and replacement. We have fabricated HA/PCL and bioactive glass/PCL composite 3D scaffolds for bone regeneration, and Ti 3D scaffolds for bone replacement by the layer manufacturing process, and have characterized in vitro and in vivo biocompatibilities, such as compressive modulus, proliferation of osteoblast-like MG63 cells, differentiation of hBMSC, bioactivity in simulated body fluid, and bony implantation with tibial, calvarial and mastoid defect models using rabbits and rats.

Osteogenic cell proliferation and differentiation were good on HA/PCL and bioactive glass/PCL composite 3D scaffolds. Nano-size of HA was more effective to facilitate initial cell attachment than micro-size of HA, owing to hydrophilicity of HA and very high specific surface area of nano particles exposed on the scaffold surface. Likewise, mesoporous bioactive glass showed better cell attachment and proliferation compared with conventional bioactive glass because of high specific surface area and beneficial ion release for bony cell proliferation. Implantation of HA/PCL 3D scaffolds in rabbit tibia and mastoid obliteration in rat model showed excellent bone ingrowth and regeneration inside the scaffold. Ti 3D scaffolds exhibited higher mechanical strength than ceramic/polymer composite scaffolds, which might be suitable for load bearing bone replacement. Surface modification of Ti 3D scaffolds leaded to good bioactivity in simulated body fluid. Pore structure of 3D scaffolds also influenced mechanical properties and biocompatibility

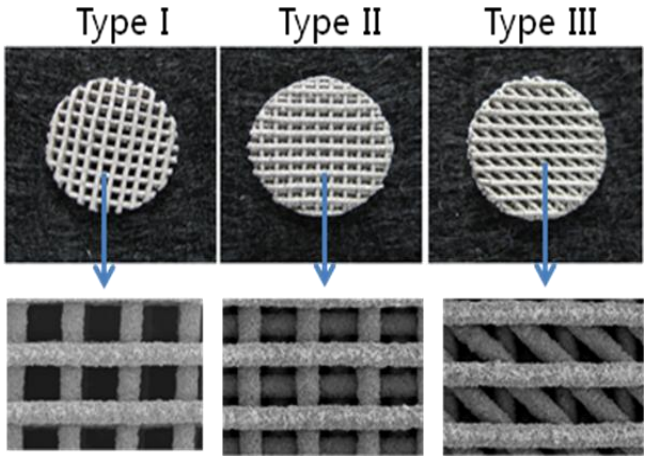

<3D scaffolds with different pore structure>

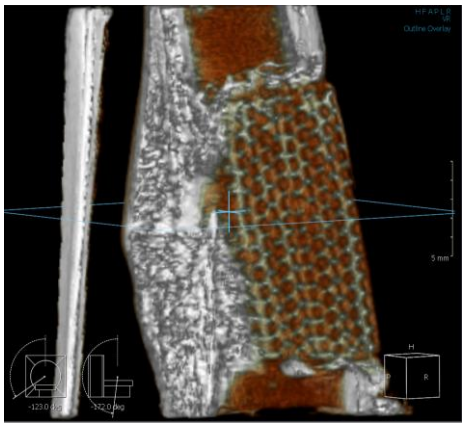

<Micro-CT image of implantation>

Deformation measurement of bone model with a dental implant by DIC

Yasuyuki Morita[1], Yasuyuki Matsushita[2], Mitsugu Todo[3], Kiyoshi Koyano[2]
1 *Graduate School of Engineering, Nagoya University*
2 *Graduate School of Dental Science, Kyushu University*
3 *Research Institute for Applied Mechanics, Kyushu University*
morita@mech.nagoya-u.ac.jp

Introduction

Recently, dental implants have become important in odontotherapy since they dramatically improve a patient's quality of life by restoring the functions of mastication, speech, and sensuousness diminished by lost teeth or periodontium. However, postoperative complications, such as bone resorption and dental implant fracture, can arise from inappropriate treatment. Many studies have examined the role of mechanical problems in these postoperative complications, but due to experimental difficulties, few studies have investigated the strain and stress distributions in bones resulting from placing dental implants. Most such studies have used numerical analyses, such as the finite element method. Experimentally, the photoelasticity technique can be applied to visualize the stress distribution of a photoelastic polymer monolayer. In general, however, bone consists of a bilayer structure comprising cortical and cancellous bone.

Therefore, this study examined sawbones laminated test blocks, which have a structure close to that of bone. Fixtures were implanted in bone models that simulated bilayer cortical and cancellous bone. A cross-sectional surface was exposed by cutting the specimen with a universal milling machine to observe the fixture/bone interface. Then, we analyzed the displacement and strain distributions in the boundary area under simulated dental occlusion conditions using a digital image correlation (DIC) method. In this study, we compared the displacement/strain distributions between osseointegrated implant and unosseointegrated implant specimens. In the unosseointegrated implant specimen, the fixture which is a component of a dental implant did not adhere to the bone model, since it was simply implanted in the model. Then, the interface simulated an immediate-loaded implantology, which has recently come into widespread use, in which the implant does not adhere to bone in the early stage. On the other hand, in the osseointegrated implant specimen, the fixture adhere to the bone model with adhesive.

Experimental Method

Specimen geometry and manufacture method Sawbones laminated test blocks were used as a bone model to simulate actual bilayer bone consisting of cortical and cancellous alveolar bone. The cortical and cancellous bone specimens were made from glass-reinforced epoxy and solid polyurethane, respectively. The mechanical properties of this phantom bone model are similar to those of actual bone. Each specimen measured 40×40×30 mm^3, and the cortical bone was 2 mm thick at both ends. Tapered fixtures (POI EX FINAFIX POI47-14TP-L; JMM Corp.) were used in this study. The maximum outside diameter, total length, and bone-implanted length of this fixture were 4.7 mm, 16 mm, and 14 mm, respectively.

Specimens were constructed in the following manner: Holes were drilled in the bone model block using the drills specified by JMM. The holes were accurately created using a universal milling machine (2MF-U; Hitachi Seiki) to reduce the individual differences among specimens. Then, a fixture was implanted manually in each hole by self-tapping with a tapping wrench with adhesive (6004N; Sumitomo 3M) for osseointegrated implant specimens and without adhesive for unosseointegrated implant specimens. For the specimens with an implanted fixture, the cross-sectional surface was exposed to measure the whole-field displacement distribution.

Specimen preparation A compression test to simulate dental occlusion was performed in the fol-

lowing manner. (i) Random patterns were created on the area to be observed by spraying it with a synthetic resin, pigment, and organic solvent (S05032; Dai Nippon Toryo) for DIC analysis. (ii) The specimen was placed in a tabletop materials tester (EZ Test; Shimadzu), with a load resolution of 0.010 N and a displacement resolution of 10 μm. (iii) A compression load was applied to the top of the fixture. The pre-compression load was –4.0 N to avoid initial rigid-body movement of the specimen. (iv) The compression load, which paralleled the longitudinal axis of the fixture, was increased until it reached –200 N at a crosshead speed of 0.50 mm/min. (v) Load and displacement data were recorded throughout the loading period and digital images of the specimen surface were taken every –10 N during the continuous loading with a charge-coupled device (CCD) camera (D80; Nikon). Each image measured 2600×3900 pixels, and one pixel was equivalent to an area of 4.7×4.7 μm^2. (vi) Vic-2D (Correlated Solutions) analysis software was for the DIC method.

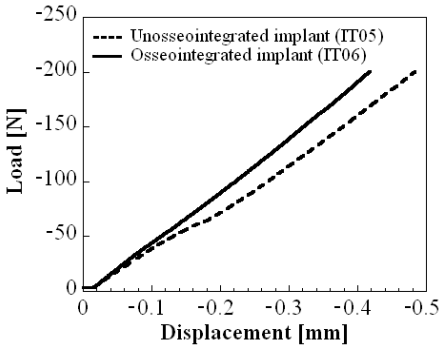

Fig. 1 Load-displacement curves.

Experimental Results and Discussion

Figure 1 shows examples of a load-displacement curve obtained in the simulated occlusion test. The horizontal and vertical axes represent the displacement of the crosshead of the material tester and the load measured with the load cell, respectively. The load was increased almost linearly with the displacement in the osseointegrated implant specimen. On the other hand, in the unosseointegrated implant specimen, the load was caused a behavior like slip at -0.15 mm of the displacement since the interface between the fixture and the bone model was not bonded with adhesive.

The strain distributions, ε_{xx}, ε_{zz}, and γ_{xz} were acquired from the displacement distribution obtained by the DIC method. The results were shown in Figs. 2 and 3, which represented the strain distributions of the unosseointegrated implant and the osseointegrated implant specimens, respectively. The location of the strain concentrations was almost same in both specimens. The ε_{xx} and γ_{xz} were concentrated in the bone at the tapered area of the fixture. The concentration of the ε_{zz} appeared in the bone at the tip of the fixture. However, the distributions were quite different. The strain distribution of the unosseointegrated implant specimen did not spread widely to the bone area, though the one of the osseointegrated implant specimen spread pretty widely to the bone area. This means that the occlusion force was supported by many bones in the osseointegrated bone specimen, the unosseointegrated specimen was not. The difference was caused by whether the interface between the bone model and the fixture was bonded or not. The maximum strain values in the unosseointegrated implant specimen were higher than in the osseointegrated implant one. The values were (ε_{xx}, ε_{zz}, γ_{xz}) = (-0.6, -5.0, 1.9%) and (-0.3, -1.5, 0.4%), respectively. This might suggest that the unosseointegrated implantology is subject to bone resorption compared to the osseointegrated one.

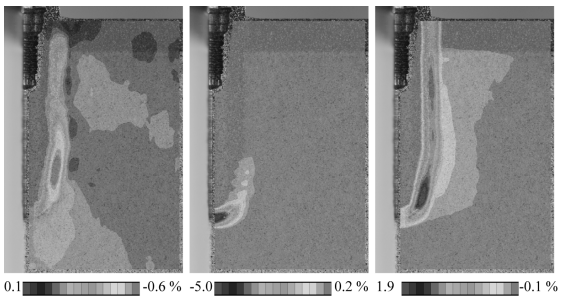

Fig. 2 Strain distributions of an unosseointegrated implant specimen.

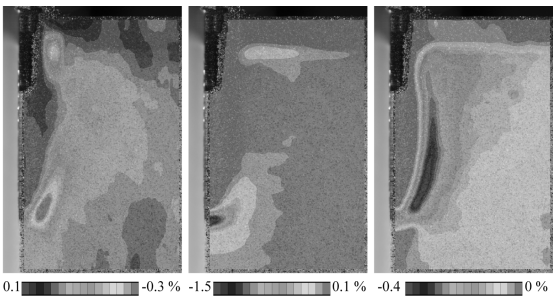

Fig. 3 Strain distributions of an osseointegrated implant specimen.

The influence of immediate loading on bone around titanium implants with different surface topographies

T. Kuwana, N. Sato, M. Yokoyama, M. Fujikawa, M.Yamamoto,
R. Uzuka, T. Anada, O.Suzuki, and K. Sasaki
Tohoku University Graduate School of dentistry, Sendai, Japan

Implant therapy is reliable treatment for missing teeth due to improved surgical techniques and development of macro and micro implant-designs. For early esthetic and functional recovery of the patients, the concept of immediate implant loading has been widely accepted; however, there is little biological evidence to support this concept.

The objective of this study was to examine the influence of immediate loading on bone formation around titanium implants with different surface topographies.

Materials and Methods: 12weeks wistar rats were anesthetized with pentobarbital (intraperitoneal injection). The titanium implants, 1.2mm in diameter and 9.25 mm in length, were prepared in two types: smooth implants and acid etched implants. Two titanium implants were inserted perpendicular to the bone surface of right tibiae of the rats. The first implant was placed 5 mm from the knee joint of the bone and the second one was placed 13mm distal form the first implant; they were parallel to each other. Subsequently, the continuous static load was applied by using 10mm closed coil springs, which produced 2N continuously.

Surface characteristics of the implants were examined by SEM and surface roughness measurement. The samples were imaged with X-ray micro-CT. The bone mineral density (BMD) and surface area between mineralized bone and the implants were analyzed using image analysis software for the micro-CT images. The biomechanical test of the implant-bone interface was examined by the removal torque test at 1, 2, and 4 weeks after loading.

Results: SEM images showed that the smooth surface was relatively smooth topography and the acid-etched surface had a uniformly 0.5-1.5 μm size compartment surrounded by sharp peaks and valleys. The average roughness (Ra) s for the smooth surface and acid-etched surface were 0.341±0.084μm and 2.223±0.264μm, respectively. No clinical mobility of the implants was observed for entire experimental period. Surface differences remarkably affected the biomechanical strength of bone-implant integration. Reverse torque values for acid etched implants were about two times greater than those for smooth implants, in addition, the loading tended to decrease reverse torque values for smooth implants. Although BMD for both implants were increased by loading at week 1 and 2, the loading appeared to decrease BMD at week 4.

Conclusion: These results suggested that immediate loading might decrease biomechanical strength of bone-implant integration for smooth implants and increase BMD for both implants at early healing period and decrease at late healing period in rats.

Application of Ni-free Ti-based Shape Memory Alloy for Maxillofacial Treatment

Hiroyasu Kanetaka[1,2], Yoshinaka Shimizu[2], Tada-aki Kudo[2], Ye Zhang[1], Mitsuhiro Kano[2], Yuya Sano[2], Hideki Hosoda[3], Shuichi Miyazaki[4] and Keiichi Sasaki[2]

1) Graduate School of Biomedical Engineering, Tohoku University

2) Graduate School of Dentistry, Tohoku University

3) Precision and Intelligence Laboratory, Tokyo Institute of Technology

4) Institute of Materials Science, University of Tsukuba

kanetaka@m.tohoku.ac.jp

1. Introduction

The unique properties of shape memory and superelasticity have made shape memory alloys (SMAs) very useful biomaterials. These properties are very advantageous for medical use, and actually the SMA wires have been widely used in medical and dental field. However, biocompatibility of nickel-titanium (Ni-Ti) alloy, which is the only practical SMA at present, has been questioned because it contains a large amount of nickel. The aim of this study was to evaluate the performance of a newly developed Ni-free Ti-based SMA wire as orthopedic or orthodontic force generator for maxillofacial treatment.

2. Materials and Methods

Orthopedic forces (expansive and compressive groups) acted on the interparietal suture in Wistar rats (male, 6 weeks old). After systemic and local anesthesia, parietal bone was exposed. Round perforations through the cranial cavity were made and Ti-Nb-Al round wires (73mol%Ti, 24mol%Nb and 3mol%Al) of 0.45mm diameter were set on both parietal bones.

For orthodontic force generator, Ti-Nb-Al or Ni-Ti round wires of 0.3mm diameter were bent into standardized shape and set in the oral cavities of Wistar rats (male, 6 weeks old), and orthodontic palatal movements of maxillary first molars were performed.

3. Results and Discussion

The interparietal suture showed an enlarged opening and thin edges in expansive group. On the other hand, the suture showed an impermeable line and thick edges in compressive group. For tooth movement, there was no significant difference in the amount of the movement between the Ti-Nb-Al and Ni-T groups. The results suggested that newly developed Ti-Nb-Al alloy had excellent mechanical properties equivalent to Ni-Ti alloy and could generate optimal orthopedic or orthodontic force for maxillofacial treatment.

Aging behavior of β-type Ti-37Nb-3Zr with super-elasticity

Qiang Li[1, 2], Mitsuo Niinomi[2], Masaaki Nakai[2] and Xianjin Yang[1]
1. School of Material Science and Engineering, Tianjin University
2. Institute for Materials Research, Tohoku University
liqiang@imr.tohoku.ac.jp

Titanium and its alloys are widely used as biomaterials because of their high strength, excellent corrosion resistance, and high biocompatibility. In the past two decades, many β-type titanium alloys, which consist of nontoxic elements such as Nb, Ta, Sn and Zr, were studies to obtain low Young's modulus or super-elasticity. Ti-29Nb-13Ta-4.6Zr (TNTZ) was designed by Niinomi's group using a molecular orbital method, which is based on two quantum parameters, the bond order (Bo) and the d-orbital energy level (Md) [1]. The former parameter, Bo, is the covalent bond strength between Ti and the alloying element. The latter parameter, Md, is related to the electro-negativity and the atomic radius of elements [2]. It has been reported that the stress-induced α" martensite transformation and its reverse transformation causes super-elasticity at room temperature [3]. This kind of super-elasticity is sensitive to chemical compositions of alloys and could be predicted by the above-mentioned method.

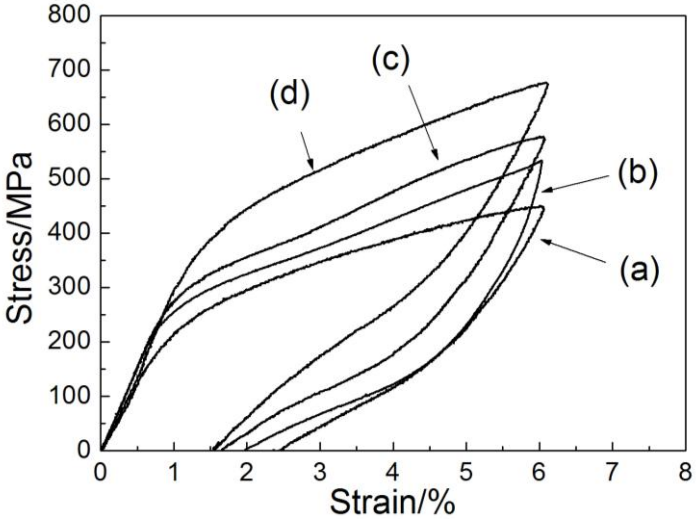

Fig.1 Loading and unloading curves of Ti-37Nb-3Zr subjected to (a) solution treatment at 1073K for 3.6ks, and aging treatment at 573K for (b) 1.8ks, (c)3.6ks and (d) 7.2ks, respectively.

In this study, Ti-37Nb-3Zr (mass%) was designed as a kind of super-elastic alloy. Under solution treatment conditions, it's total recovery strain is around 3.5% after unloading from applied strain of 6% as shown in Fig.1. However, samples were aged at 573K for different periods after solution treatment to get higher strengths. As a result, the recovery strain rises to about 4.4% accompanying with the increase in strength. The ω phase is formed during aging treatment, and it may play an important role in the enhancement of strength and super-elasticity.

1) D. Kuroda *et al.*: Mater. Sci. Eng. A, 243 (1998) 244.
2) M. Morinaga *et al.*: Titanium 1992 Science and Technology (Proc. 7th World Conf. on Titanium, San Diego, CA, USA, June 29-July 2, 1992) pp.276.
3) C. Baker: Metal Sci., 5 (1971) 92.

Glass-Structure Control in Zr-based Metallic Glasses by Varying Casting-Atmosphere Condition

Albertus D. Setyawan[1], Hidemi Kato[1], Junji Saida[2] and Akihisa Inoue[1]

[1] *Institute for Materials Research, Tohoku University, Sendai 980-8577, Japan*

[2] *Center for Interdisciplinary Research, Tohoku University, Sendai 980-8578, Japan*

alb_deny@imr.tohoku.ac.jp

Assessing glass-forming ability (GFA) of an alloy can be performed by comparing the kinetics of transformation, such as the nucleation or crystal growth rate, as well as evaluation criterion, e.g. the large of supercooled liquid region ΔT_x ($=T_x-T_g$, where T_g and T_x are the glass transition and the crystallization temperatures, respectively) or the well-known reduced glass transition temperature T_{rg} ($= T_g/T_l$, where T_l is the liquidus temperature). However, a more straight-forward method sometimes is necessary, for example by comparing the critical size for glass formation derived from the as-prepared structure of samples with various sizes. Mold-casting is a simple technique for fabricating bulk metallic glassy specimens. In this work, GFA in the $Zr_{65}Al_{7.5}Ni_{10}Cu_{17.5-x}Pd_x$ (x=0–17.5) alloy system is evaluated by mapping all the structures of alloys fabricated by mold casting.

The work is successful in unveiling the origin of different dependence of apparent GFA on casting-atmosphere-pressure (p) among the alloys in the system. It is found that low-Pd alloys (x=0–5) exhibit an apparent GFA with low dependence on p, while those with higher Pd contents (x=7.5–17.5) show an apparent GFA with a remarkably high dependence on p. The critical diameter d_c of glass formation in the 0- and 5-at.%-Pd alloys remains 6 and 5 mm, respectively, while in the 17.5-at.%-Pd one, d_c increases gradually from 1 to 5 mm as Ar atmosphere pressure rises from vacuum (p~2×10^{-3} Pa) to ambient (p~10^5 Pa). A characteristic cooling process concerning the gas species and pressure applied for casting atmosphere is observed during mold-casting. Cooling curves show a feature in which a deflection to a much lower cooling rate is exhibited when a low p is applied. The deflection takes place particularly starting at a temperature of about T_g+160 K which corresponds to the low-temperature side of undercooled liquid region. Such a characteristic is independent of alloy composition (Pd content, x). On the other hand, continuous-cooling-temperature (CCT) diagrams successfully constructed for the alloys of x=5 and x=17.5 alloys show that, for the same time scale, the former has only a CCT curve corresponding to the formation crystalline phase lying at high-temperature side of the undercooled liquid region, while the later reveals an additional CCT curve of a quasicrystalline phase formation at considerably lower temperature side. By correlating the cooling characteristic in mold casting and the continuous cooling phase transformation feature of the alloys, the origin of different dependence of GFA and as-cast structure on casting-atmosphere pressure between the low- and high-Pd sides in this alloy system can be well explained. Furthermore, based on the result, an appropriate strategy in structural control has been successfully applied for the alloy system.